

# Delocalization in harmonic chains with long-range correlated random masses

F. A. B. F. de Moura, M. D. Coutinho-Filho, E. P. Raposo  
*Laboratório de Física Teórica e Computacional, Departamento de Física,  
Universidade Federal de Pernambuco, 50670-901 Recife, PE, Brazil*

M. L. Lyra

*Departamento de Física, Universidade Federal de Alagoas, 57072-970 Maceió, AL, Brazil*

We study the nature of collective excitations in harmonic chains with masses exhibiting long-range correlated disorder with power spectrum proportional to  $1/k^\alpha$ , where  $k$  is the wave-vector of the modulations on the random masses landscape. Using a transfer matrix method and exact diagonalization, we compute the localization length and participation ratio of eigenmodes within the band of allowed energies. We find extended vibrational modes in the low-energy region for  $\alpha > 1$ . In order to study the time evolution of an initially localized energy input, we calculate the second moment  $M_2(t)$  of the energy spatial distribution. We show that  $M_2(t)$ , besides being dependent of the specific initial excitation and exhibiting an anomalous diffusion for weakly correlated disorder, assumes a ballistic spread in the regime  $\alpha > 1$  due to the presence of extended vibrational modes.

PACS numbers: 63.50.+x, 63.22.+m, 62.30.+d

## I. INTRODUCTION

The role played by disorder on the nature of collective excitations in condensed matter physics has been the subject of intensive studies due to its relevance in defining general transport characteristics [1]. Usually, disorder induces localization of collective excitations thus degrading transport properties, an effect that is largely pronounced in low dimensions. In particular, the one-electron eigen-states in the one-dimensional Anderson model with site-diagonal uncorrelated disorder are exponentially localized for any degree of disorder [2]. However, several one-dimensional models with correlated disorder have been proposed which exhibit delocalized states [3, 4, 5]. Recently, it has been shown that the one-dimensional Anderson model with long-range correlated disorder presents a phase of extended electronic states [6, 7, 8]. These results have been confirmed by microwave transmission spectra of single-mode waveguides with inserted correlated scatters [9].

The above results have motivated the study of further model systems that can be mapped onto the Anderson model and, therefore, expected to present a similar transition between localized and extended collective excitations. Recently, a study concerning the one-dimensional quantum Heisenberg ferromagnet with exchange couplings exhibiting long-range correlated disorder reported some finite-size scaling evidences of the emergence of a phase of extended low-energy excitations [10]. By using a renormalization group calculation the existence of such phase of extended spin-waves was confirmed and the scaling of the mobility edge with the degree of correlation was obtained [11]. It was also shown that, associated with the emergence of extended spin-waves in the low-energy region, the wave-packet mean-square displacement exhibits a long-time ballistic behavior.

The collective vibrational motion of one-dimensional disordered harmonic chains of  $N$  random masses can also

be mapped onto an one-electron tight-binding model [12]. In such a case, most of the normal vibrational modes are localized. However, there are a few low-frequency modes not localized, whose number is of the order of  $\sqrt{N}$ , in which case the disordered chains behaves like the disorder-free system [12, 13]. Futher, it was shown that correlations in the mass distribution produce a new set of non-scattered modes in this system [14]. Non-scattered modes have also been found in disordered harmonic chain with dimeric correlations in the spring constants [15]. By using analytical arguments, it was also demonstrated that the transport of energy in mass-disordered (uncorrelated and correlated) harmonic chains is strongly dependent on non-scattered vibrational modes as well as on the initial excitation [16]. For impulse initial excitations, uncorrelated random chains have a superdiffusive behavior for the second moment of the energy distribution [ $M_2(t) \propto t^{1.5}$ ], while for initial displacement excitations a subdiffusive spread takes place [ $M_2(t) \propto t^{0.5}$ ]. The dependence of the second moment spread on the initial excitation was also obtained in Ref. [17]. Moreover, correlations induced by thermal annealing have been shown to enhance the localization length of vibrational modes, although they still present an exponential decay for distances larger than the thermal correlation length [18]. Recently the thermal conductivity on harmonic and anharmonic chains of uncorrelated random masses [19], as well as of the chain of hard-point particles of alternate masses [20], has been numerically investigated in detail. The main issue here is whether the systems display finite thermal conductivity in the thermodynamic limit, a question that remains controversial [21].

In this paper we extend the study of collective modes in the presence of long-range correlated disorder for the case of vibrational modes. We will consider harmonic chains with long-range correlated random masses assumed to have spectral power density  $S \propto 1/k^\alpha$ . By using a transfer matrix calculation, we obtain accurate estimates for

the Lyapunov exponent, defined as the inverse of the degree of localization  $\lambda_c$  of the vibrational modes. We show that, for  $\alpha > 1$ , this model also presents a phase of extended modes in the low frequency region. This result is confirmed by participation ratio measurements from an exact diagonalization procedure and finite size scaling arguments. The spatial evolution of an initially localized excitation is also studied by computing the spread of the second moment of the energy distribution,  $M_2(t)$ . We find that, associated with the emergence of a phase of delocalized modes, a ballistic energy spread takes place.

## II. FORMALISM

We consider a disordered harmonic chain of  $N$  masses, for which the equation of motion for the displacement  $u_n$  of the  $n$ -th mass with vibrational frequency  $\omega$  is [13, 14]

$$(\beta_{n-1} + \beta_n - \omega^2 m_n)u_n = \beta_{n-1}u_{n-1} + \beta_n u_{n+1} \quad . \quad (1)$$

Here  $m_n$  is the mass at the  $n$ -th site and  $\beta_n$  is the spring constant that couples the masses  $m_n$  and  $m_{n+1}$ . We use units in which  $\beta_n = 1$ . In the present harmonic chain model, we take the masses  $m_n$  following a random sequence describing the trace of a fractional Brownian motion [22, 23, 24]:

$$m_n = \sum_{k=1}^{N/2} \left[ k^{-\alpha} \left( \frac{2\pi}{N} \right)^{(1-\alpha)} \right]^{1/2} \cos \left( \frac{2\pi n k}{N} + \phi_k \right), \quad (2)$$

where  $k$  is the wave-vector of the modulations on the random mass landscape and  $\phi_k$  are  $N/2$  random phases uniformly distributed in the interval  $[0, 2\pi]$ . The exponent  $\alpha$  is directly related to the Hurst exponent  $H$  ( $\alpha = 2H + 1$ ) of the rescaled range analysis. In order to avoid vanishing masses we shift and normalize all masses generated by Eq. (2) such to have average value  $\langle m_n \rangle = 5$  and variance independent of the chain size ( $\langle \Delta m_n \rangle \equiv 1$ ).

Using the matrix formalism, Eq. (1) can be rewritten as

$$\begin{pmatrix} u_{n+1} \\ u_n \end{pmatrix} = \begin{pmatrix} 2 - m_n \omega^2 & -1 \\ 1 & 0 \end{pmatrix} \begin{pmatrix} u_n \\ u_{n-1} \end{pmatrix}. \quad (3)$$

For a specific frequency  $\omega$ , a  $2 \times 2$  transfer matrix  $T_n$  connects the displacements at the sites  $n - 1$  and  $n$  to those at the site  $n + 1$ :

$$T_n = \begin{pmatrix} 2 - m_n \omega^2 & -1 \\ 1 & 0 \end{pmatrix}. \quad (4)$$

Once the initial values for  $u_0$  and  $u_1$  are known, the value of  $u_n$  can be obtained by repeated iterations along the chain, as described by the product of transfer matrices

$$Q_N = \prod_{n=1}^N T_n. \quad (5)$$

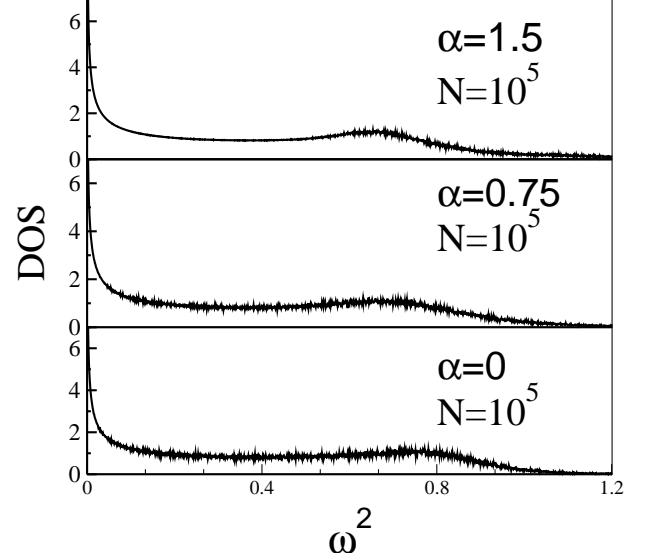


FIG. 1: Normalized density of states (DOS) as a function of  $\omega^2$  obtained using Dean's method. The chain length is  $N = 10^5$  for all cases. The DOS becomes less rough as  $\alpha$  is increased. For  $\alpha = 1.5$  it displays a non-fluctuating part near the bottom of the band.

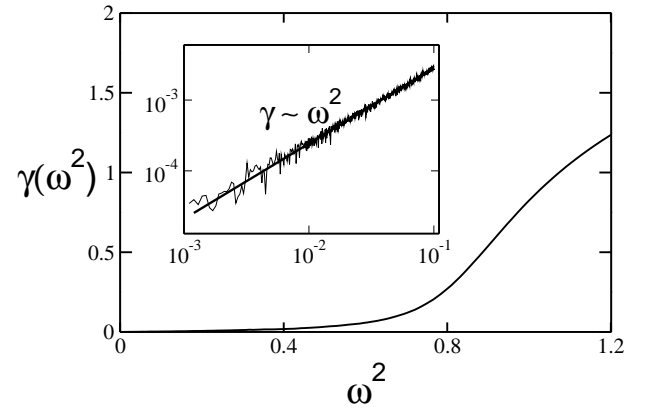


FIG. 2: Lyapunov coefficient  $\gamma$  as a function of  $\omega^2$  for  $\alpha = 0$  (uncorrelated random chain) and  $N = 2 \times 10^5$  sites. The Lyapunov coefficient is finite for non-zero frequencies (localized states) and vanishes as  $\gamma \propto \omega^2$ ,  $\omega \rightarrow 0$  (inset).

The localization length of each vibrational mode is taken as the inverse of the Lyapunov exponent  $\gamma$  defined by [13, 14, 25]

$$\gamma = \lim_{N \rightarrow \infty} \frac{1}{N} \log \frac{|Q_N c(0)|}{|c(0)|}, \quad (6)$$

where  $c(0) = \begin{pmatrix} u_1 \\ u_0 \end{pmatrix}$  is a generic initial condition. Typically,  $2 \times 10^5$  matrix products were used to calculate the Lyapunov exponents. The nature of the vibrational modes can also be investigated by computing the participation ratio  $\xi$ , since it displays a dependence on the chain size for extended states and is finite for exponentially local-

ized ones.  $\xi$  is defined by [15, 18]

$$\xi(\omega) = \frac{\sum_{n=1}^N u_n^2}{\sum_{n=1}^N u_n^4}, \quad (7)$$

where the displacements  $u_n$  are those associated with an eigenmodes  $\omega$  of a chain of  $N$  masses and are obtained by direct diagonalization of the  $N \times N$  secular matrix  $A$  defined by  $A_{i,i} = (\beta_i + \beta_{i-1})/m_i = 2/m_i$ ,  $A_{i,i+1} = A_{i+1,i} = \beta_i^2/(m_i m_{i+1}) = 1/(m_i m_{i+1})$ , and all other  $A_{i,j} = 0$  [12, 14]. The participation ratio calculations were averaged over 100 samples.

We compute the Lyapunov exponents and the participation ratio for several values of the correlation exponent  $\alpha$ , and obtain the density of states (DOS) using the numerical Dean's method [26]. Strong fluctuations in the DOS are related to the presence of localized states, whereas smooth a DOS is usually connected with the emergence of delocalized states [5, 14]. In Fig. 1 we show the normalized DOS for chains with  $N = 10^5$  sites, and notice that it becomes less rough as  $\alpha$  is increased. In Fig. 2 we display the plot of  $\gamma$  versus  $\omega^2$  for  $\alpha = 0$  (uncorrelated random masses). The Lyapunov coefficient is finite for all frequencies and vanishes at  $\omega = 0$  as  $\gamma \propto \omega^2$ , in agreement with Ref. [13] (see inset of Fig. 2). The scaled participation ratio  $\xi/N$  as a function of  $\omega^2$  is shown in Fig. 3:  $\xi(\omega^2 = 0)/N$  remains finite in the thermodynamic limit, whereas for any finite frequency the vibrational modes are localized with  $\xi/N \rightarrow 0$  as  $N \rightarrow \infty$ , in agreement with the above results obtained from the Lyapunov coefficient calculations. To investigate the effect of weak long-range correlated disorder, we present in Fig. 4(a) the Lyapunov coefficient as a function of  $\omega^2$  for  $\alpha = 0.75$  and  $N = 2 \times 10^5$ . In spite of  $\gamma$  being very small in the bottom of the band, the scaled participation ratio for  $\omega > 0$  vanishes in the thermodynamic limit [see Fig. 4(b)]. Therefore, all modes with  $\omega > 0$  are still localized, a feature that holds for any  $0 \leq \alpha \leq 1$ . However, the nature of the low-frequency modes changes qualitatively for  $\alpha > 1$ . In Fig. 5(a) we show  $\gamma$  versus  $\omega^2$  for  $\alpha = 1.5$  and  $N = 2 \times 10^5$  sites. The Lyapunov coefficient vanishes within a finite range of frequency values, thus revealing the presence of extended vibrational modes. The scaled participation ratio  $\xi/N$  [see Fig. 5(b)] displays a well defined data collapse, confirming that the phase of extended low-frequency vibrational modes is stable in the thermodynamic limit.

### III. ENERGY TRANSPORT

In order to study the time evolution of a localized energy pulse, we calculate the second moment of the energy distribution [16, 17]. This quantity is related to the thermal conductivity by Kubo's formula [16, 27]. The classical Hamiltonian  $H$  for an harmonic chain can be written

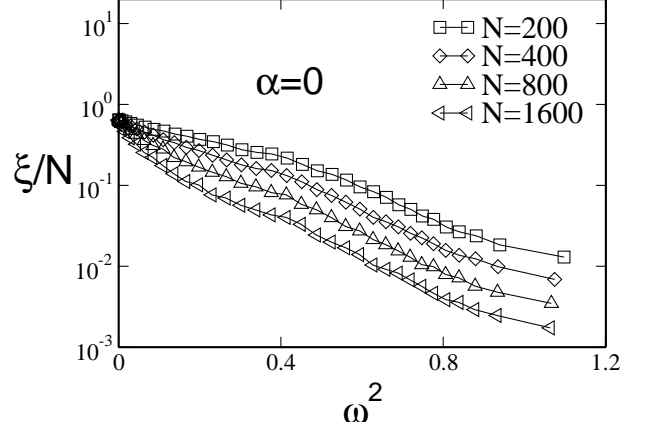


FIG. 3: Scaled participation ratio  $\xi/N$  as a function of  $\omega^2$  for  $\alpha = 0$  (uncorrelated disorder). From top to bottom,  $N = 200, 400, 800, 1600$ . For vibrational modes with  $\omega > 0$ ,  $\xi/N \rightarrow 0$  as  $N$  diverges, thus confirming their localized nature.

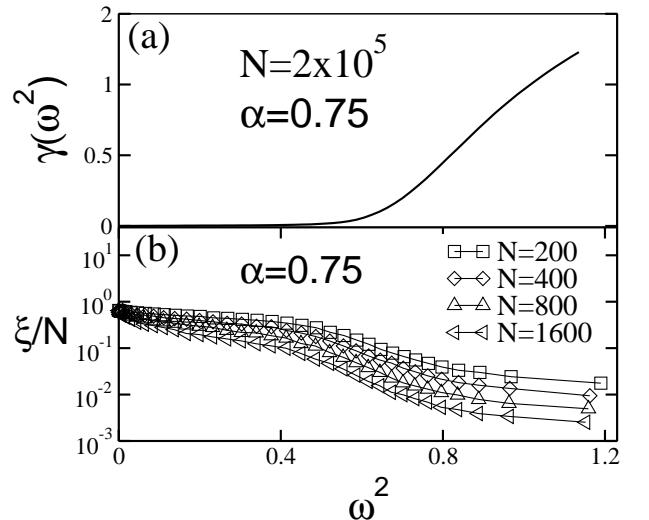


FIG. 4: (a) Lyapunov coefficient  $\gamma$  versus  $\omega^2$  for  $\alpha = 0.75$  and  $N = 2 \times 10^5$  sites. (b) Scaled participation ratio  $\xi/N$  as a function of  $\omega^2$  for  $\alpha = 0.75$ . From top to bottom,  $N = 200, 400, 800, 1600$ . In spite of  $\gamma$  being very small in the bottom of the band, all modes with  $\omega > 0$  are localized.

as

$$H = \sum_{n=1}^N h_n(t), \quad (8)$$

where the energy  $h_n(t)$  at the site  $n$  is given by

$$h_n(t) = \frac{P_n^2}{2m_n} + \frac{\beta_n}{4}[(Q_{n+1} - Q_n)^2 + (Q_n - Q_{n-1})^2]. \quad (9)$$

Here  $P_n$  and  $Q_n$  define the momentum and displacement of the mass at the  $n$ -th site. The Hamilton's equations are

$$\dot{P}_n(t) = -\frac{\partial H}{\partial Q_n} = \beta_n[(Q_{n+1} - Q_n) - (Q_n - Q_{n-1})] \quad (10)$$

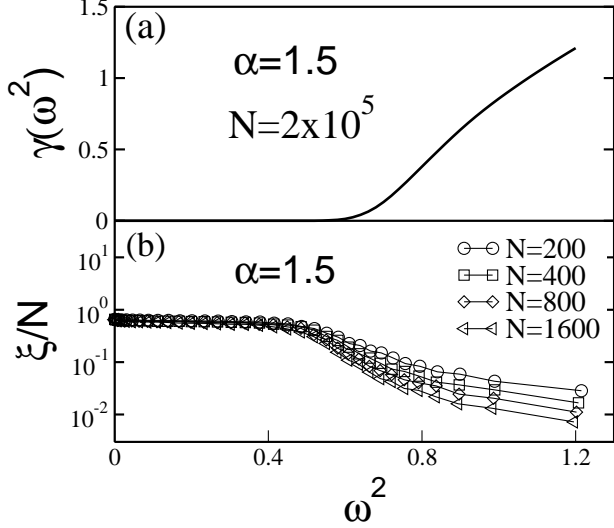


FIG. 5: (a) Lyapunov coefficient  $\gamma$  versus  $\omega^2$  for  $\alpha = 1.5$  and  $N = 2 \times 10^5$  sites. The Lyapunov coefficient vanishes within a finite range of frequency values, thus revealing the presence of extended vibrational modes. (b) Scaled participation ratio  $\xi/N$  as a function of  $\omega^2$  for  $\alpha = 1.5$ . From top to bottom,  $N = 200, 400, 800, 1600$ . The phase of extended vibrational modes is confirmed by the size independent plateau in the low-frequency region.

and

$$\dot{Q}_n(t) = \frac{\partial H}{\partial P_n} = \frac{P_n(t)}{m_n} . \quad (11)$$

The fraction of the total energy  $H$  at the site  $n$  is given by  $h_n(t)/H$  and the second moment of the energy distribution,  $M_2(t)$ , is defined by [16]

$$M_2(t) = \sum_{n=1}^N (n - n_0)^2 [h_n(t)/H], \quad (12)$$

where an initial excitation is introduced at the site  $n_0$  at  $t = 0$ . Using the fourth-order Runge-Kutta method, we solve the differential equations for  $P_n(t)$  and  $Q_n(t)$  and calculate  $M_2(t)$ . The second moment of the energy distribution  $M_2(t)$  has the same status of the mean-square displacement of the wavepacket of an electron in a crystal [16]. In harmonic chains with an initial impulse excitation, the energy spread is faster than that in chains with an initial displacement excitation [16, 17]. We calculate  $M_2(t)$  for several  $\alpha$  values and two kinds of initial excitation: impulse excitation and displacement excitation.

### A. Impulse excitation

In Fig. 6 we present the scaled second moment  $M_2(t)/t^{1.5}$  versus time  $t$  for  $\alpha = 0$  (dotted line), which corresponds to the uncorrelated random chain, and  $\alpha =$

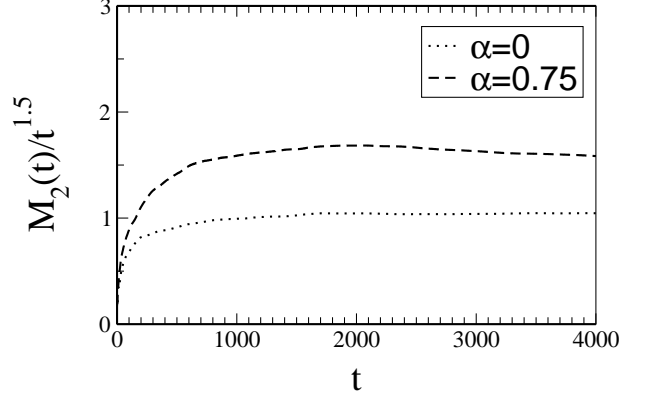


FIG. 6: Scaled energy second moment  $M_2(t)/t^{1.5}$  versus time  $t$  for  $\alpha = 0$  (dotted line) and  $\alpha = 0.75$  (dashed line) with initial impulse excitation. For  $0 \leq \alpha \leq 1$  only superdiffusive behavior is found for long times.

0.75 (dashed line). These results have been obtained after an initial impulse excitation,  $P_{n_0}(t = 0) = \delta_{n_0, N/2}$ . In our calculations for  $\alpha = 0$ , the self-expanded chain method with initial chain size  $N = 1000$  was used to minimize end effects. Throughout the numerical integration process we kept the fraction of the total energy  $H$  at the ends of the chain  $[h_0(t)/H$  and  $h_N(t)/H]$  smaller than  $10^{-300}$  for all times. As shown in Fig. 6, we find a long-time superdiffusive behavior for  $\alpha = 0$ , in agreement with previous analytical and numerical results for energy transport in harmonic chains with uncorrelated random masses under an impulse initial excitation [16]. In contrast, for  $\alpha > 0$  we cannot use the self-expanded chain method due to the long-range character of the mass correlations. Therefore, chains with  $N = 10000$  masses were considered, and the runs stopped whenever the fraction of the total energy at the chain ends achieved  $10^{-300}$ . For  $\alpha = 0.75$  the time-dependence of the scaled energy second moment  $M_2(t)/t^{1.5}$  typically represents a weak long-range correlated case. In such a case we also find superdiffusive behavior for long times. On the other hand, in the strong correlated regime,  $\alpha > 1$ , a breakdown in the superdiffusive behavior sets up. Fig. 7 shows the time-dependence of the scaled energy second moment,  $M_2(t)/t^2$ , for  $\alpha = 1.5$  (dotted line) and  $\alpha = 2.0$  (dashed line). Associated with the emergence of extended vibrational modes in the low-energy region, the second moment  $M_2(t)$  displays a long-time ballistic behavior.

### B. Displacement excitation

The long time behavior of the second moment  $M_2(t)$  in uncorrelated random chains with initial displacement excitation is significantly different from the corresponding behavior with impulse initial excitation [16, 17]. Analytical calculations predict that  $M_2(t) \propto t^{0.5}$ , a result that has been corroborated by numerical techniques [16]. For

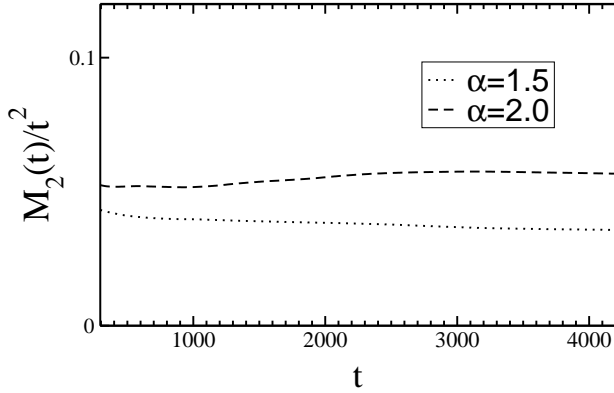


FIG. 7: Scaled second moment  $M_2(t)/t^2$  versus time  $t$  for  $\alpha = 1.5$  (dotted line) and  $\alpha = 2.0$  (dashed line) with initial impulse excitation. Results were obtained by numerical integration in chains with  $N = 10000$  sites. A ballistic behavior is found after an initial transient.

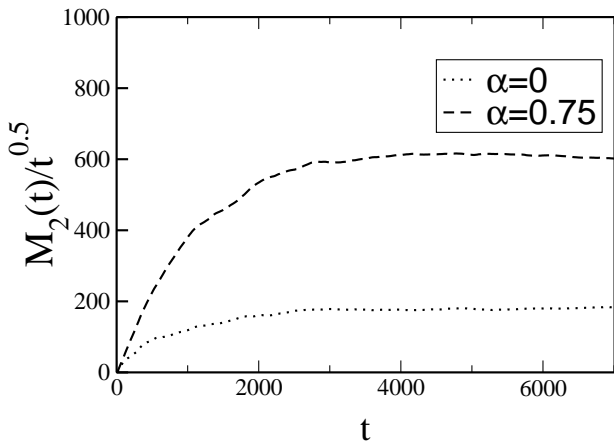


FIG. 8: The scaled second moment  $M_2(t)/t^{0.5}$  versus time  $t$  for  $\alpha = 0$  (dotted line) and  $\alpha = 0.75$  (dashed line) with initially given displacement excitation. The subdiffusive behavior is found for long times.

$\alpha = 0$  we indeed reproduce this behavior, as shown in Fig. 8 for the scaled second moment  $M_2(t)/t^{0.5}$  versus time  $t$  with initial displacement excitation  $Q_{n_0}(t = 0) = \delta_{n_0, N/2}$ . Again, we find that this asymptotic subdiffusive behavior remains true for  $0 \leq \alpha < 1$  (dashed line in Fig. 8). For strong correlations ( $\alpha > 1$ ), which induce the emergence of new extended vibrational modes in the low-energy region, the energy transport is faster than in the subdiffusive regime and again assumes a ballistic nature, as shown in Fig. 9.

#### IV. SUMMARY AND CONCLUSIONS

In this paper we have studied the nature of collective vibrational modes in harmonic chains with long-range correlated random masses  $m_n$ , with spectral power density  $S \propto 1/k^\alpha$ . By using a transfer matrix method

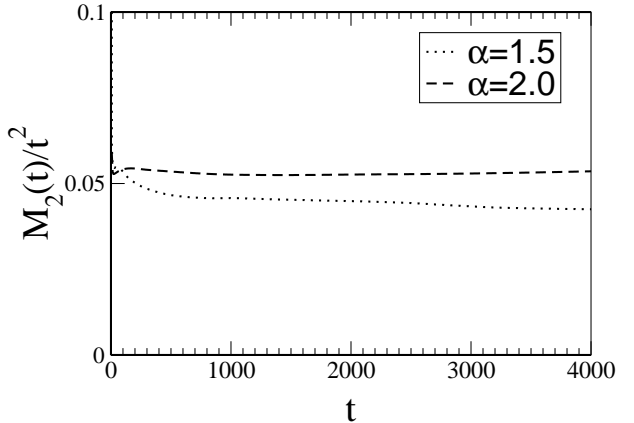


FIG. 9: The scaled second moment  $M_2(t)/t^2$  versus time  $t$  for  $\alpha = 1.5$  (dotted line) and  $\alpha = 2.0$  (dashed line) with initially given displacement excitation. Results obtained by numerical integration of differential equation for chain with  $N = 10000$  sites. A ballistic behavior is found for all times.

and exact diagonalization, we have computed the localization length and the participation ratio of all normal modes. Our results indicate that in the strong correlations regime,  $\alpha > 1$ , there is a phase of extended low-energy vibrational modes. In this sense, long-range correlations in the mass distribution induce the emergence of a delocalization transition in harmonic chains similar to the one observed to occur with one-magnon excitations in ferromagnetic chains with random couplings [10, 11] and with one-electron eigen-states in the random hopping Anderson model [7]. We have also studied the energy transport in this harmonic chain model. The spread of the energy second moment  $M_2(t)$  is shown to be strongly dependent on the existence of non-scattered vibrational modes and initial excitation. We have also found that, associated with the emergence of a phase of low-energy extended collective excitations,  $M_2(t)$  displays a crossover from an anomalous sub- or super-diffusive regime (depending on the initial impulse or displacement excitation, respectively) to an asymptotic ballistic behavior. The above findings indicate that the thermal conductivity can be strongly influenced by the presence of long-range correlations in the random distribution of masses and we hope that the present work will stimulate further studies along this direction.

#### V. ACKNOWLEDGMENTS

This work was partially supported by CNPq, CAPES and FINEP (Brazilian agencies). MLL also acknowledges the partial support of FAPEAL (Alagoas state agency).

---

[1] T. A. L. Ziman, Phys. Rev. Lett. **49**, 337 (1982). For a review see, e.g., B. Kramer and A. MacKinnon, Rep. Prog. Phys. **56** 1469, (1993).

[2] E. Abrahams, P. W. Anderson, D. C. Licciardello, and T. V. Ramakrishnan, Phys. Rev. Lett. **42**, 673 (1979). For a review see, e.g., I. M. Lifshitz, S. A. Gredeskul and L. A. Pastur, *Introduction to the Theory of Disordered Systems* (Wiley, New York, 1988).

[3] J. C. Flores, J. Phys.: Condens. Matter **1**, 8471 (1989).

[4] D. H. Dunlap, H. L. Wu, and P. W. Phillips, Phys. Rev. Lett. **65**, 88 (1990); H.-L. Wu and P. Phillips, Phys. Rev. Lett. **66**, 1366 (1991); P. W. Phillips and H.-L. Wu, Science **252**, 1805 (1991);

[5] S. N. Evangelou and D. E. Katsanos, Phys. Lett. A **164**, 456 (1992). See also, S. N. Evangelou, A. Z. Wang, and S. J. Xiong, J. Phys.: Condens. Matter **6**, 4937 (1994).

[6] F. A. B. F. de Moura and M. L. Lyra, Phys. Rev. Lett. **81**, 3735 (1998).

[7] F. A. B. F. de Moura and M. L. Lyra, Physica A **266**, 465 (1999).

[8] F. M. Izrailev and A. A. Krokhin, Phys. Rev. Lett. **82**, 4062 (1999); F. M. Izrailev, A. A. Krokhin, and S. E. Ulloa, Phys. Rev. B **63**, 41102 (2001).

[9] U. Kuhl, F. M. Izrailev, A. Krokhin, and H. J. Stöckmann, Appl. Phys. Lett. **77**, 633 (2000).

[10] R. P. A. Lima, M. L. Lyra, E. M. Nascimento, and A. D. de Jesus, Phys. Rev. B **65**, 104416 (2002).

[11] F. A. B. F. de Moura, M. D. Coutinho-Filho, E. P. Raposo and M. L. Lyra, Phys. Rev. B, **66**, 014418 (2002).

[12] P. Dean, Proc. Phys. Soc. **84**, 727 (1964).

[13] H. Matsuda and K. Ishii, Prog. Theor. Phys. Suppl. **45**, 56 (1970); K. Ishii, Prog. Theor. Phys. Suppl. **53**, 77 (1973).

[14] P. K. Datta and K. Kundu, J. Phys.: Condens. Matter **6**, 4465 (1994).

[15] F. Dominguez-Adame, E. Macià and A. Sánchez, Phys. Rev. B **48**, 6054 (1993).

[16] P. K. Datta and K. Kundu, Phys. Rev. B **51**, 6287 (1995).

[17] M. Wagner, G. Zart, J. Vazquez-Marquez, G. Viliani, W. Frizzera, O. Pilla, and M. Montagna, Philos. Mag. B **65**, 273 (1992).

[18] J. C. Cressoni and M. L. Lyra, Phys. Rev. B **53**, 5067 (1996); J. Phys.: Condens. Matter **8**, L83 (1996).

[19] B. Li, H. Zhao and B. Hu, Phys. Rev. Lett. **86**, 63 (2001); A. Dhar, Phys. Rev. Lett. **86**, 5882 (2001);

[20] P. L. Garrido, P. I. Hurtado and B. Nadrowski, Phys. Rev. Lett. **86**, 5486 (2001); A. V. Savin, G. P. Tsironis and A. V. Zolotaryuk, Phys. Rev. Lett. **88**, 154301-1 (2002).

[21] A. Dhar, Phys. Rev. Lett. **88**, 249401-1 (2002); P. L. Garrido and P. I. Hurtado, Phys. Rev. Lett. **88**, 249402-1 (2002).

[22] J. Feder, *Fractals* (Plenum Press, New York, 1988); A. Tsoularis, *Chaos: From Theory to Applications* (Plenum Press, New York, 1992).

[23] A. R. Osborne and A. Provenzale, Physica D **35**, 357 (1989).

[24] N. P. Greis and H. S. Greenside, Phys. Rev. A **44**, 2324 (1991).

[25] S. N. Evangelou and E. N. Economou, J. Phys. A: Math. Gen. **26**, 2803 (1993).

[26] P. Dean, Rev. Mod. Phys. **44**, 127 (1972).

[27] P. B. Allen and J. L. Feldman, Phys. Rev. B **48**, 12581 (1993).